Optimal Tap Setting of Voltage Regulation Transformers in Unbalanced Distribution Systems

Brett A. Robbins, *Student Member, IEEE*, Hao Zhu, *Member, IEEE*,
and Alejandro D. Domínguez-García, *Member, IEEE*

***Abstract*—In this paper, we propose a method to optimally set the tap position of voltage regulation transformers in distribution systems. We cast the problem as a rank-constrained semidefinite program (SDP), in which the transformer tap ratios are captured by (i) introducing a secondary-side 'virtual' bus per transformer, and (ii) constraining the values that these virtual bus voltages can take according to the limits on the tap positions. Then, by relaxing the non-convex rank-1 constraint in the rank-constrained SDP formulation, one obtains a convex SDP problem. The tap positions are determined as the ratio between the primary-side bus voltage and the secondary-side virtual bus voltage that result from the optimal solution of the relaxed SDP, and then rounded to the nearest discrete tap values. To efficiently solve the relaxed SDP, we propose a distributed algorithm based on the Alternating Direction Method of Multipliers (ADMM). We present several case studies with single- and three-phase distribution systems to demonstrate the effectiveness of the distributed ADMM-based algorithm, and compare its results with centralized solution methods.**

***Index Terms*—Transformers, Relaxation Methods, Distributed Algorithms, Decentralized Control, Power System Analysis Computing**

I. Introduction

In power distribution systems, tap-changing under-load (TCUL) transformers are commonly used for regulating voltage. Traditionally, automatic voltage regulators (AVRs) are utilized to control the transformer tap position based on local voltage measurements (see e.g., [1], [2]). While this AVR-based control is effective in achieving local voltage regulation, it is likely not optimal in terms of achieving certain overall system operational objectives, e.g., minimize power losses and voltage regulation from some reference value. Motivated by this, we propose a framework to determine the transformer tap ratios in distribution systems that is optimal in some sense.

To address the problem described above, we formulate an optimal power flow (OPF), where the transformer tap ratios are included as decision variables and the objective is to minimize the total power losses (although, other objectives can be accomplished as well). In the context of transmission systems, optimal transformer tap setting under the OPF framework has been investigated for decades. For example, in [3], the transformer tap positions are included as discrete variables in the OPF problem, which results in a mixed-integer program (MIP) formulation. Unfortunately, the computational complexity of this formulation grows exponentially as the number of transformers increases, and thus becomes intractable for large systems. To tackle this complexity issue, several papers have proposed to relax transformer tap positions to continuous optimization variables, and then the solutions to the closest discrete valuables (see e.g., [3]–[5]). This alternative approach can yield acceptable performance without incurring the added complexity. However, all of these approaches are restricted to standard OPF formulations, and are known to potentially suffer from the same convergence issues present in traditional iterative solvers.

In this paper, we formulate the OPF problem that arises in the context of voltage regulation in distribution systems as a rank-constrained semidefinite program (SDP), and subsequently obtain a convex SDP problem from the original SDP formulation by dropping the only non-convex rank-1 constraint (see, e.g., [6]–[9]). In general, this rank relaxation is not guaranteed to attain the global minimum, in particular for mesh networks. Interestingly, it has been shown that under some mild conditions, the optimal solution for the relaxed SDP-based OPF problem turns out to be of rank 1 for tree-structured networks, which are typical of radial distribution systems [6]–[8]. In this sense, the rank relaxation scheme is actually guaranteed to attain the global optimum of the original OPF problem. In addition to handling the OPF problem, the SDP-based approach also constitutes a very promising tool to tackle the non-convexity in other monitoring and control applications in power distribution systems.

It is possible to extend the SDP-based OPF approach to include the tap ratios of TCUL transformers by introducing a virtual secondary-side bus per transformer, which in turn will result in additional constraints and decision variables [10]–[12]. However, the TCUL transformer model proposed in [11] is limited due to two issues: (i) the relaxed SDP problem could fail to yield a rank-1 solution, and thus its global optimality is no longer guaranteed; and (ii) it is only applicable to single-phase systems. The first issue arises since the network is equivalently broken into two disconnected parts by introducing virtual buses associated to each transformer, and the network disconnection would lead to multiple solutions of rank 2 [12]. Although an optimal rank-1 solution could be recovered in this case, the conditions for recovering rank-1 solutions are only possible for single-phase systems [11], [12]. As for the second issue, it is well known that distribution systems are unbalanced; this motivates the formulation of the three-phase OPF problem [9]. As it will become more clear later

B. A. Robbins, H. Zhu, and A. D. Domínguez-García are with the Department of Electrical and Computer Engineering, University of Illinois at Urbana-Champaign, Urbana, IL, 61801. E-mail: {robbins3, haozhu, aledan}@ILLINOIS.EDU.

This material is based upon work supported by ABB under project "Distributed and Resilient Voltage Control of Distributed Energy Resources in the Smart Grid" (University of Illinois contract UIeRA 2013-2955-00-00).

on, it is impossible to enforce the phase separation between the primary- and secondary-side buses for the transformer model in [11]. To address this issue, we propose an alternative transformer model by including a highly resistive line between the primary- and secondary-side buses. The proposed method does not introduce additional complexity as compared to [11], but can successfully resolve the two aforementioned issues. Related to our approach, [13] and [14] discuss adding a very small resistance term to the model to handle a similar network disconnection issue due to the presence of ideal transformers. It is worth pointing out that such a method will maintain phase angles between primary- and secondary-side buses, but will return incorrect power transfers; hence it is not deemed effective for modeling transformers.

In order to solve the relaxed SDP problem described earlier, rather than using iterative solvers traditionally used to solve the OPF problem, we are interested in fast distributed solvers to handle the higher computational complexity introduced by the SDP formulation. Distributed methods for solving the OPF problem have been proposed in power systems in a variety of contexts (see, e.g., [7], [9], [15] and the references therein). In particular, the Alternating-Direction Method of Multipliers (ADMM) has been widely used as a simple, yet powerful technique for solving distributed convex optimization problems [16]. This method has been successfully applied in power systems for the dispatch of distributed generation and deferrable loads [9], [15], as well as state estimation [17]. In this paper, we leverage the ADMM to solve the relaxed SDP-based optimal tap problem in a distributed fashion. The ability to perform the optimization tasks in parallel can dramatically reduce computation time and complexity, especially for large-scale systems [15]. Note that the proposed distributed solver can be implemented in a distributed environment or solved centrally and parallelized across several processors.

In this paper, we do not consider the real/reactive power settings of distributed energy resources (DERs) as optimization variables since this is covered extensively in [7]–[9]. However, we could easily incorporate the setting of these devices into our framework as decision variables and modify the constraints and objective function as appropriate. In practice, we envision a two time-scale architecture that categorizes devices as either slow or fast time-scale devices with the idea of controlling them separately. Conventional voltage regulation devices, e.g., TCUL transformers, would be considered slow time-scale devices, whereas power electronic interfaced DERs would be the latter. Then, given that fast (and uncontrolled) changes in DER active generation (consumption) might cause the voltage to deviate from some reference voltage, a second optimization [7] or a feedback control scheme [18], executed at regular intervals (e.g., every minute), could be utilized to determine the active/reactive power setting of controllable DERs. These two time-scale separation ideas have been suggested in [7] and we intend to explore them further.

The remainder of this paper is organized as follows. Section II introduces the system model and formulates the transformer tap-setting optimization problem. In Section III, we rewrite the OPF as a convex SDP, and introduce a modified transformer model that will allow us to extend this framework to a three-phase unbalanced system. The distributed solver is given in Section IV. Section V presents the case studies and concluding remarks are presented in Section VI.

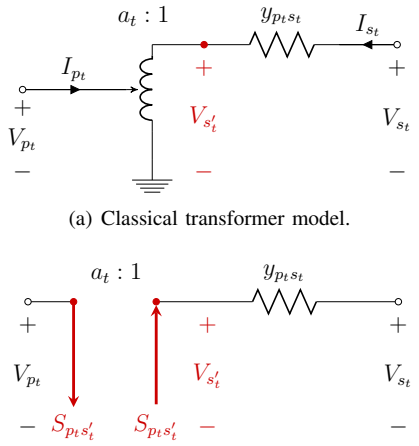

(a) Classical transformer model.

(b) Equivalent transformer model.

Figure 1: Tap-changing under load transformer models

II. Problem Formulation

In this section, we first introduce the standard TCUL transformer model in the literature. Then, we describe the power system model adopted in this work and formulate the single-phase optimal power flow (OPF) problem that includes the transformer tap positions as decision variables.

A. Standard Transformer Model

Figure 1(a) shows the standard model of the t^{th} TCUL transformer located on the distribution line segment (p_t, s_t) of some distribution system. Without loss of generality, we assume that the primary side of the transformer is closest to the feeder head, and the admittance for the attached distribution line segment(s) and core losses (which are typically ignored in distribution systems [1], [19]) are referred to the secondary side as $y_{p_t s_t}$. Given the tap ratio a_t, this model contains an *ideal* transformer directly connected to bus p_t and the virtual secondary-side bus s'_t such that $V_{p_t} = a_t V_{s'_t}$. The tap ratio a_t is a discrete variable that typically takes on 33 possible values $\{\tilde{a}_{-16}, \ldots, \tilde{a}_0, \ldots, \tilde{a}_{16}\}$, uniformly distributed around $\tilde{a}_0$ to create a specified range around the rated voltage of the transformer (which corresponds to $\tilde{a}_0$). For instance, the taps can move up and down 16 positions from the nominal tap ratio $\tilde{a}_0 = 1$ with each step corresponding to $5/8\%$ p.u. change. With the typical nominal voltage at 1 p.u., the tap ratio is bounded by $\underline{a} = \tilde{a}_{-16} = 0.9$ and $\overline{a} = \tilde{a}_{16} = 1.1$ [2]. Then, the line current and bus voltage relationships for the circuit in Fig. 1(a), which depend nonlinearly on the tap ratio, are

$$\begin{bmatrix} I_{p_t} \\ I_{s_t} \end{bmatrix} = \begin{bmatrix} y_{p_t s_t}/a_t^2 & -y_{p_t s_t}/a_t \\ -y_{p_t s_t}/a_t & y_{p_t s_t} \end{bmatrix} \begin{bmatrix} V_{p_t} \\ V_{s_t} \end{bmatrix}. \quad (1)$$

Figure 1(b) shows an equivalent model to the one in Fig. 1(a) that removes the *ideal* transformer entirely and augments the network with the virtual bus s'_t. We treat the

buses p_t and s'_t as though they are electrically disconnected and introduce an additional variable $S_{p_t s'_t}$ to account for the power transferred across the removed ideal transformer, e.g., buses p_t and s'_t will have a net injection of $-S_{p_t s'_t}$ and $S_{p_t s'_t}$, respectively. Unlike the model in (1), the primary/secondary power is independent of the tap ratio. The key advantages of this alternative model are that: (i) the tap ratio is only necessary in order to define the secondary-side bus voltage as $V_{s'_t} = V_{p_t}/a_t$, and (ii) the admittance matrix for the equivalent circuit will remain constant. Hence, in the remainder of the paper we will use the primary/secondary power relationship of the alternative transformer model in Fig. 1(b). Note that transformers with fixed turn ratios are easily incorporated by modifying the admittance matrix Y as described by (1).

B. Power System Model

Consider an n-bus power system that has r TCUL transformers. Let $\mathcal{T} := \{1, \dots, r\}$ denote the set of transformers. The set of buses incident to the primary-side of a transformer is defined as $\mathcal{N}_p := \{p_t \,|\, t \in \mathcal{T}\}$; similarly, for buses incident to the secondary side, we have that $\mathcal{N}_s := \{s_t \,|\, t \in \mathcal{T}\}$. Additionally, the set of virtual buses (introduced in the equivalent transformer model in Fig. 1(b)) is defined as $\mathcal{N}_{s'} := \{s'_t \,|\, t \in \mathcal{T}\}$. The remaining m system buses define the set $\mathcal{N}_b := \{1, 2, \dots, m\}$. Thus, the set of physical buses will be

$$\mathcal{N} = \mathcal{N}_b \cup \mathcal{N}_p \cup \mathcal{N}_s, \tag{2}$$

and the set of buses in the augmented network created by adding the virtual buses is

$$\mathcal{N}_a = \mathcal{N} \cup \mathcal{N}_{s'}, \tag{3}$$

where $|\mathcal{N}_a| = n + r$.

The edge-set that represents the set of distribution line segments (which could contain conductors for single-, two-, or three-phase circuits) is $\mathcal{E} \subseteq \mathcal{N}_a \times \mathcal{N}_a$ such that $(i,k) \in \mathcal{E}$ is the distribution line between buses i and k. The admittance matrix for the single-phase network $Y \in \mathbb{C}^{(n+r)\times(n+r)}$ will reflect the topology of the augmented network. Furthermore, we define the set $S_{ps'} := \{S_{p_t s'_t} \,|\, t \in \mathcal{T}\}$ as the power transferred through the transformers. This balanced single-phase model will be extended to the general unbalanced three-phase case in Section III-D.

Finally, in order to include the equivalent transformer model in Fig. 1(b), the power flow equations will be formulated depending on the type of bus as follows:

1) No transformer incident to a bus: Consider the case when there are no transformers incident to bus i. Let $\mathcal{H}_i := \{i\} \cup \{k \,|\, (i,k) \in \mathcal{E}\}$ be the set of buses electrically connected to bus i, which has no transformers incident to it. Then, the power injected in bus i is

$$S_i = S_i^g - S_i^d = \sum_{k \in \mathcal{H}_i} [Y^*]_{ik} V_i V_k^*, \ \forall i \in \mathcal{N} \backslash \mathcal{N}_p, \tag{4}$$

where the generation S_i^g and load S_i^d are positive quantities.

2) Transformer incident to a bus: As shown in Fig. 1(b), we track the power across the transformer via $S_{p_t s'_t}$, and capture the tap ratio with the voltage relationship $V_{s'_t} = V_{p_t}/a_t$. If bus i is incident to the primary-side of a transformer, then the corresponding power flow equation becomes

$$S_{p_t} - S_{p_t s'_t} = \sum_{k \in \mathcal{H}_{p_t}} [Y^*]_{p_t k} V_{p_t} V_k^*, \ \forall t \in \mathcal{T}, \tag{5}$$

or, for the virtual secondary-side bus, we have that

$$S_{p_t s'_t} = \sum_{k \in \mathcal{H}_{s'_t}} [Y^*]_{s'_t k} V_{s'_t} V_k^*, \ \forall t \in \mathcal{T}. \tag{6}$$

Note that the secondary-side buses in $\mathcal{N}_s$ are no longer directly incident to transformers as in the circuit model in Fig. 1(a).

C. Transformer Tap Ratio Optimization

Next, we formulate an OPF problem, the solution of which will provide the tap settings of the TCUL transformer in the network. As mentioned earlier, the discrete tap positions lead to an MIP formulation and its complexity grows exponentially with the number of TCUL transformers [3]. To tackle this, we relax the values that the discrete transformer tap ratio $a_t \in \{\underline{a}, \dots \overline{a}\}$ can take, and allow a_t to take values on the continuous interval $[\underline{a}, \overline{a}]$. Once the optimal a_t is obtained, it will be rounded to the closest discrete value in $\{\underline{a}, \dots, \overline{a}\}$.

Given some operational objective function $f(V, a)$, which we describe in detail later in Section III-C, defined over the system voltages $V \in \mathbb{C}^{n+r}$, and by letting tap ratios $a \in \mathbb{R}^r$ denote the vector of transformer tap ratios, the OPF problem of interest can be formulated as follows:

$$\min_{V,\, a,\, S_{ps'}} f\left(V, a, S_{ps'}\right) \tag{7a}$$

such that

$$\sum_{k \in \mathcal{H}_i} [Y^*]_{ik} V_i V_k^* - S_i = 0, \ \forall i \in \mathcal{N} \backslash \mathcal{N}_p \tag{7b}$$

$$\sum_{k \in \mathcal{H}_{p_t}} [Y^*]_{p_t k} V_{p_t} V_k^* - S_{p_t} + S_{p_t s'_t} = 0, \qquad \forall t \in \mathcal{T} \tag{7c}$$

$$\sum_{k \in \mathcal{H}_{s'_t}} [Y^*]_{s'_t k} V_{s'_t} V_k^* - S_{p_t s'_t} = 0, \qquad \forall t \in \mathcal{T} \tag{7d}$$

$$V_{p_t} - a_t V_{s'_t} = 0, \qquad \forall t \in \mathcal{T} \tag{7e}$$

and

$$\underline{V} \leq \left|V_i\right| \leq \overline{V}, \quad \forall i \in \mathcal{N} \tag{7f}$$

$$\underline{a} \leq \ a_t \ \leq \overline{a}, \quad \forall t \in \mathcal{T}. \tag{7g}$$

The high granularity of the available tap positions enables the continuous tap-ratio representation approach to yield acceptable results without incurring the added complexity of an MIP formulation [3]–[5]. However, the optimization problem in (7) is still challenging due to the nonlinearity in the power flow equations, as captured by constraints (7b)-(7d). Hence, the ensuing section will introduce additional relaxations to handle these nonlinearities in the power flow model.

III. Convex Relaxation

In this section, we first reformulate the non-convex OPF problem in (7) into matrix form. Then, we review a modified transformer model that we proposed in [12]; this model will allow us to handle three-phase unbalanced OPF. Finally, we use the modified transformer model to develop the convex relaxation of the matrix-based OPF formulation in (7).

A. Matrix-Based OPF Formulation

Motivated by the convex relaxation approach in [10]–[12], we will reformulate (7) as an equivalent semidefinite program (SDP). To this end, the complex power injection at bus $i \in \mathcal{N}$ is given by

$$S_i = V_i \sum_{k \in \mathcal{H}_i} [Y^*]_{ik} V_k^*, \tag{8}$$

where $S, V \in \mathbb{C}^{n+r}$. We define $W \in \mathbb{C}^{(n+r)\times(n+r)}$ as

$$W = VV^H = \begin{bmatrix} V_1^2 & \cdots & V_1 V_{n+r}^* \\ \vdots & \ddots & \vdots \\ V_1^* V_{n+r} & \cdots & V_{n+r}^2 \end{bmatrix}, \tag{9}$$

where W is a positive semidefinite (PSD) matrix ($W \succeq \mathbf{0}$) with rank 1. Interestingly, the complex power in (8) is linearly related to the entries of W as follows:

$$S_i = \mathrm{Tr}\left(H_i W\right), \tag{10}$$

with $H_i := Y^H E_i$, where $E_i := e_i e_i^{\mathrm{T}}$ and e_i is a vector with all entries equal to zero except the i^{th} one that is equal to one. Furthermore, the complex power flowing from bus i to k over line $(i,k) \in \mathcal{E}$ is given by

$$S_{ik} = \mathrm{Tr}\left(A_{ik} W\right), \tag{11}$$

where $A_{ik} := -e_k^{\mathrm{T}} Y^H e_i E_{ik}$ and $E_{ik} := (e_i - e_k)\, e_i^{\mathrm{T}}$.

We remove the tap ratio from the voltage relationship in (7e) and (7g) by constraining the voltage on the secondary-side of the transformer relative to the primary side, i.e.,

$$\underline{a}^2 V_{p_t}^2 \le V_{s_t'}^2 \le \overline{a}^2 V_{p_t}^2. \tag{12}$$

Therefore, the equivalent matrix formulation of the problem in (7) is as follows:

$$\min_{W \succeq \mathbf{0},\, S_{ps'}} f(W) \tag{13a}$$

such that

$$\mathrm{Tr}\left(H_i W\right) - S_i = 0, \quad \forall i \in \mathcal{N} \backslash \mathcal{N}_p \tag{13b}$$

$$\mathrm{Tr}\left(H_{p_t} W\right) - S_{p_t} + S_{p_t s_t'} = 0, \quad \forall t \in \mathcal{T} \tag{13c}$$

$$\mathrm{Tr}\left(H_{s_t'} W\right) - S_{p_t s_t'} = 0, \quad \forall t \in \mathcal{T} \tag{13d}$$

and

$$\underline{V}^2 \le [W]_{ii} \le \overline{V}^2, \quad \forall i \in \mathcal{N} \tag{13e}$$

$$\underline{a}^2 [W]_{p_t p_t} \le [W]_{s_t' s_t'} \le \overline{a}^2 [W]_{p_t p_t}, \quad \forall t \in \mathcal{T} \tag{13f}$$

and

$$[W]_{p_t s_t'} = [W]_{s_t' p_t} \ge 0, \quad \forall t \in \mathcal{T} \tag{13g}$$

$$\mathrm{rank}(W) = 1. \tag{13h}$$

The constraint (13g) ensures that V_{p_t} and $V_{s_t'}$ have the same phase angle. Once the solution to (13) is obtained, the tap ratio a_t of transformer t can be determined using the bus voltage ratio as follows:

$$a_t = \sqrt{V_{p_t}^2 / V_{s_t'}^2} = \sqrt{[W]_{p_t p_t} / [W]_{s_t' s_t'}}\ . \tag{14}$$

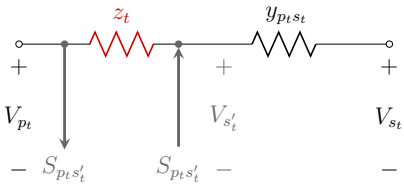

Figure 2: Non-ideal transformer model.

B. Non-ideal Transformer Model

As it will be discussed in detail in Section III-C, the optimization problem in (13) can be relaxed to a convex one by dropping the rank-1 constraint [7]–[9]. For distribution networks, it has been shown in [7] that this relaxation approach would yield a rank-1 solution; therefore, achieving the global optimum of the original problem. As pointed out in [12], the transformer model in Fig. 1(b) results in two electrically disconnected networks. Accordingly, it has been shown that the solution to the relaxed problem could be of higher-rank, albeit with no loss of optimality as compared to the original problem. However, the higher-rank solution leads to an arbitrary phase angle difference between the primary-side bus and downstream buses. Such phase angle ambiguity would significantly complicate the analysis of the three-phase system, since the angle separation among the three phases can no longer be enforced at the virtual secondary bus.

The issue discussed here can be resolved by introducing the modified transformer model shown in Fig. 2, where we place an impedance z_t between p_t and s_t' of the ideal transformer introduced earlier to 're-connect' the network. Choosing an appropriate value of z_t will ensure that the power flow in the modified model almost mimics that of an electrically disconnected network. As detailed later, this modification would help maintain the phase angle consistency on both sides of the transformer; i.e., $\theta_{p_t} \approx \theta_{s_t'}$. This is highly attractive since it allows one to solve an equivalent convex formulation of the original OPF problem in (7), while enforcing the correct phase shift for the transformers. This is especially important to extend the OPF framework to three-phase systems where the phase separation is lost with the disconnected network.

As discussed in detail in Section V-C, we found via numerical simulations that there can be a large range of values for z_t that yield solutions that are sufficiently accurate. However, if $|z_t|$ is too small, the augmented network admittance matrix Y could be problematic as the entries corresponding to (p_t, s_t') become much larger compared to the rest. Although a small $|z_t|$ maintains $\theta_{p_t} \approx \theta_{s_t'}$, the power flow through z_t will become comparable to $S_{p_t s_t'}$, and thus the system power flow would be different from the original ideal transformer model. On the other hand, if $|z_t|$ becomes too large, then the system behavior begins to mirror the original disconnected case with ideal transformers. The latter scenario will result in a solution

W that has a rank greater than one. The value of $|z_t|$ needs to be chosen within a specific range, which can vary based on the system and the gains in the cost function. Interestingly, all of our numerical simulations corroborated that a z_t with a resistance value of several orders of magnitude (around 2-4 orders for our test systems) larger than the neighboring distribution line segments yielded the best results.

C. Rank-Relaxed Convex OPF

We apply the modifications to the transformer model as described in Section III.B and relax the rank-1 constraint in (13) to get a rank-relaxed convex OPF of the form:

$$\min_{W \succeq \mathbf{0},\, S_{ps'}} f\left(W\right) \tag{15a}$$

such that

$$\text{Tr}\left(\tilde{H}_i W\right) - S_i = 0, \quad \forall i \in \mathcal{N} \backslash \mathcal{N}_p \tag{15b}$$

$$\text{Tr}\left(\tilde{H}_{p_t} W\right) - S_{p_t} + S_{p_t s'_t} = 0, \qquad \forall t \in \mathcal{T} \tag{15c}$$

$$\text{Tr}\left(\tilde{H}_{s'_t} W\right) - S_{p_t s'_t} = 0, \qquad \forall t \in \mathcal{T} \tag{15d}$$

and

$$\underline{V}^2 \leq \ [W]_{ii} \ \leq \overline{V}^2, \qquad \forall i \in \mathcal{N} \tag{15e}$$

$$\underline{a}^2 \left[W\right]_{p_t p_t} \leq [W]_{s'_t s'_t} \leq \overline{a}^2 \left[W\right]_{p_t p_t}, \quad \forall t \in \mathcal{T}, \tag{15f}$$

where $\tilde{H}$ incorporates the non-ideal transformer model and (13g) is dropped since the network is connected. The rank-relaxed SDP formulation in (15) is guaranteed to achieve the global optimality of the non-convex tap setting problem with the rank constraint.

The objective function $f(W)$ includes a term that captures system losses, which is necessary to ensure that a rank-1 solution can be obtained from the relaxed problem [7]–[9], [11]. It may also include additional terms to capture voltage tracking objectives and power factor targets. The discussion above can be formalized by considering an objective function of the form

$$f(W) = f_0(W) + \sum_i f_i(W), \tag{16}$$

where

$$f_0\left(W\right) = \sum_{i \in \mathcal{N}_a} \sum_{k \in \mathcal{H}_i} \text{Re}\left\{\text{Tr}\left(\tilde{A}_{ik} W\right)\right\}, \tag{17}$$

which captures the total losses of all distribution line segments. The additional penalty terms in (16), $\sum_i f_i(W)$, could be chosen so as to achieve other objectives of interest; next, we discuss a few possible choices.

If a given a network has considerable distributed generation, minimizing line losses may not reduce the total demand at the (sub)transmission substation. This can be easily addressed by including a penalty term in (16) of the form

$$f_1(W) = \alpha \, \text{Re}\left\{\text{Tr}\left(\tilde{H}_{fdr} W\right)\right\}, \tag{18}$$

where α is a positive weighting factor.

Additionally, to minimize voltage magnitude deviations from a specified V_i^{ref}, we can include a penalty term in (16) of the form

$$f_2(W) = \sum_{i \in \mathcal{N}} w_i \left((V_i^{ref})^2 - [W]_{ii}\right)^2, \tag{19}$$

where $\{w_i\}$ are the positive weighting factors per bus i [20]. The weights themselves should be chosen based on: (i) the distance between the bus and the feeder, and (ii) buses that are prone to voltage violations. Intuitively, buses near the end of the (sub)laterals should be weighted more than these near the feeder in traditional radial distribution networks of unidirectional power flow.

Finally, utilities aim at operating distribution systems with a unity power factor at the feeder head. Motivated by this, the reactive reactive power injection to the feeder head bus can be penalized by

$$f_3(W) = \beta \, \text{Im}\left\{\text{Tr}\left(\tilde{H}_{fdr} W\right)\right\}, \tag{20}$$

where β is a positive weighting factor.

Note that the candidate cost functions introduced are separable among all the buses, this will facilitate the development of the distributed solver as detailed soon in Section IV.

D. Extension to Three-Phase Unbalanced Systems

So far, we assumed balanced operation, which reduced the system model to a per-phase equivalent; however, distribution systems are inherently unbalanced with untransposed distribution lines and have single-, two-, and three-phase radial feeds; therefore, a three-phase system extension of the ideas discussed so far is well motivated. The authors in [9] discuss extending the SDP relaxation OPF approach to three-phase unbalanced systems; our work focuses on incorporating three-phase TCUL transformers into such formulation. For a single-phase system, a rank-1 exact solution can be recovered even though the relaxed OPF in (13), the formulation of which is based on the ideal transformer model in Fig. 1(b), has higher-rank solutions. The additional constraints on the transformer (13g) will ensure a zero phase angle difference between the primary- and secondary-side bus voltages of that particular phase; however, the phase angles of buses downstream of the secondary-side bus are not dependent on the primary side of the transformer. In a multi-phase network, this implies that there is no constraint that enforces the angle difference between phases, i.e., $\theta_a - \theta_b \approx 120^\circ$. We can maintain this phase separation by:

(i) reconnecting the network by using the non-ideal transformer model we propose in Section III-B, or
(ii) constraining the off-diagonal entries of the submatrices $W_{p_t p_t}$ and $W_{s'_t s'_t}$ associated with the primary and secondary sides of the transformer.

The issue with (ii) is that the constraints turn out to be highly non-linear in W, which impedes us from incorporating them into the SDP OPF formulation in (15), which is why we chose to pursue solution (i).

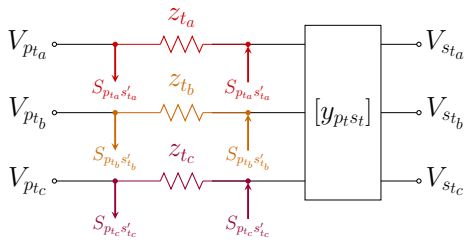

Figure 3: Equivalent three-phase transformer model.

Consider the three-phase TCUL model in Fig. 3; we will follow a configuration similar to the one used for the non-ideal transformer model in Section III-B. The core losses of the transformer will be neglected [1], and we will assume that each phase can independently regulate its secondary-side virtual bus voltage. This will be equivalent to a collection of single-phase transformers that we describe using the model in Fig. 2, which are coupled by the secondary-side distribution line admittance $y_{p_t s_t} \in \mathbb{C}^{3\times 3}$. Note that there is no mutual impedance between the primary-side bus and the virtual secondary-side virtual bus. Thus, we can optimize every tap individually and maintain the proper phase separation. We will use V_{i_a}, V_{i_b}, V_{i_c} to distinguish the voltages phasors for each phase at bus i. We also define a vector $V_{3\phi}$ that will include the voltage phasors for all the buses in the network that has at most $3 \times (n + r)$ elements if every bus has three-phase circuits. The bus voltage subindex allows one to maintain the notational consistency with the earlier single-phase (one-line) case. The only difference lies in that the dimension of the counterpart vectors to accommodate the three phases. For example, the three-phase line admittance is a block $y_{ik} \in \mathbb{C}^{3\times 3}$, as compared to $y_{ik} \in \mathbb{C}$ for single-phase cases. This way, all the analysis and problem formulation so far carries over by defining $W_{3\phi} = V_{3\phi} V_{3\phi}^H$. The power flow equations will remain unchanged where we have an (in)equality constraint per phase; however, the mutual impedances of the untransposed lines makes it more complicated to compute the line losses compared to (17). To this end, let $\tilde{e}_i \in \mathbb{N}^{|V_{3\phi}|}$ be the vector with all entries equal to zero except the entries corresponding to each phase present at bus i are set to one. Define the matrices G and K as

$$G = \text{diag}(\tilde{e}_1) Y^H \text{diag}(\tilde{e}_2) + \text{diag}(\tilde{e}_2) Y^H \text{diag}(\tilde{e}_1) \tag{21}$$

and

$$[K]_{ij} = \begin{cases} -1, & [\tilde{e}_{1_p}]_i = [\tilde{e}_{2_p}]_j = 1,\ p = \{a, b, c\} \\ 1, & i = j, \\ 0, & \text{otherwise}, \end{cases} \tag{22}$$

where $\tilde{e}_{i_p}$ is the vector $\tilde{e}_i$ conditioned on phase p, i.e., the vector contains a single nonzero entry corresponding to the entry for phase p of bus i. Thus, we update the line loss coefficient matrix A_{ik} with

$$A_{ik} = GK \tag{23}$$

to capture the total losses across each distribution line segment.

IV. Distributed Solver

It is well known that centralized algorithms for solving the SDP problem in (13) are not suitable for large systems (see, e.g., [16]). To address this issue, we propose the use of the Alternating Direction Method-of-Multipliers (ADMM), which allows for an efficient distributed solution to the convex SDP problem in (15). The ADMM is proven to be a powerful distributed optimization method and offers many benefits [16]. In particular, with ADMM, the complexity of the SDP problem scales with the sub-area size rather than with the full network size, and the communication architecture is simpler than that of a centralized scheme. Suppose we partition the system into two areas; Fig. 4 shows a topographical view of the submatrices $W^{(1)}$, $W^{(2)}$ and the boundary conditions $W^{(1,2)} = W^{(2,1)}$. The computational complexity per iteration using the popular interior point method for our SDP problem (15) scales with the fourth-order in the size of matrix W, or equivalently the number of system buses (see, e.g., [21]). For large systems, small partitions will provide significant savings in the number of optimization variables as depicted by the empty off-diagonal blocks in Fig. 4; however, the increased number of boundary conditions will require more super-iterations for convergence to a solution.

ADMM iteratively minimizes the augmented Lagrangian over three types of variables: (i) the *primary* variables, i.e., the bus voltages and transformer power transfers; (ii) the *auxiliary* variables that are used to enforce boundary conditions among neighboring areas; and (iii) the *multipliers* for dualizing the relaxed problem. The Lagrangian is designed to be separable relative to each type of variable so that we can cyclically minimize with respect to one variable type while fixing the others. This allows us to solve the problem distributedly and achieve convergence to the same solution obtained with a centralized solver [16].

We begin by partitioning the system into $\mathcal{P} := \{1, 2 \ldots, L\}$ areas such that $\cup_{i=1}^{L} \mathcal{A}^{(i)} = \mathcal{N}_a$, $\cap_{i=1}^{L} \mathcal{A}^{(i)} = \emptyset$, and $|\mathcal{A}^{(i)}| \geq 1$ for all i. To include the coupled buses, each area $\mathcal{A}^{(i)}$ needs to be augmented, and the extended area is $\bar{\mathcal{A}}^{(i)} := \mathcal{A}^{(i)} \cup \{y \,|\, (x, y) \in \mathcal{E}, x \in \mathcal{A}^{(i)}, y \in \mathcal{A}^{(j)}, i \neq j\}$. Then, the neighbors of area $\bar{\mathcal{A}}^{(i)}$ are defined as $\mathcal{M}^{(i)} := \{j \,|\, \bar{\mathcal{A}}^{(i)} \cap \bar{\mathcal{A}}^{(j)} \neq \emptyset\}$. For area $\bar{\mathcal{A}}^{(i)}$, let $W^{(i)} \in \mathbb{C}^{|\bar{\mathcal{A}}^{(i)}| \times |\bar{\mathcal{A}}^{(i)}|}$ denote the corresponding local matrix for the outer product of the bus voltages, e.g., the $|\bar{\mathcal{A}}^{(i)}| \times |\bar{\mathcal{A}}^{(i)}|$ submatrix of W corresponding to area i.

To enforce consistency between partitions, boundary conditions are required to constrain the submatrices $W^{(i,j)} = W^{(j,i)} \in \mathbb{C}^{2\times 2}$ for single phase ($\mathbb{C}^{6\times 6}$ for three phase)

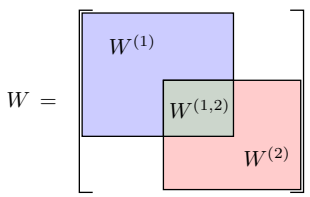

Figure 4: Partitioned system variables.

$$\mathcal{L}_c\left(\cdot\right)=\sum_{i\in\mathcal{P}}\Bigg\{f^{(i)}\left(W^{(i)}\right)+\sum_{k\in\mathcal{M}^{(i)}}\Bigg[\text{Tr}\left(\left(\Gamma^{(i,j)}\right)^{\text{T}}\left(\text{Re}\left\{W^{(i,j)}\right\}-R^{(i,j)}\right)\right)+\frac{c}{2}\left\|\text{Re}\left\{W^{(i,j)}\right\}-R^{(i,j)}\right\|_F^2 \\ +\text{Tr}\left(\left(\Lambda^{(i,j)}\right)^{\text{T}}\left(\text{Im}\left\{W^{(i,j)}\right\}-X^{(i,j)}\right)\right)+\frac{c}{2}\left\|\text{Re}\left\{W^{(i,j)}\right\}-X^{(i,j)}\right\|_F^2\Bigg]\Bigg\} \tag{25}$$

associated with the overlap between neighboring areas. We define the auxiliary variables for the boundary conditions of the local optimization as $E^{(i,j)}, F^{(i,j)} \in \mathbb{R}^{2\times 2}$ (similarly $\mathbb{R}^{6\times 6}$ for the three-phase case). These variables $E^{(i,j)}$ ($F^{(i,j)}$) are used to enforce the real (imaginary) part of the submatrix equality boundary condition on bus voltages. Note that without the auxiliary variables, our problem would not be separable with respect to each $W^{(i)}$.

For each area we also define $\mathcal{B}^{(i)}$, which captures the set of sub-matrices that satisfy the local power flow and voltage constraints described in (15b)-(15f) for area $\bar{\mathcal{A}}^{(i)}$. Given that all of the cost functions in Section III-C are separable per area, we can rewrite the global minimization problem in (15) as

$$\min_{W^{(i)}\succeq\mathbf{0}} \quad \sum_{i\in\mathcal{P}} f^{(i)}\left(W^{(i)}\right) \tag{24a}$$

such that

$$W^{(i)}\in\mathcal{B}^{(i)},\ \forall i\in\mathcal{P}, \tag{24b}$$

and

$$\text{Re}\left\{W^{(i,j)}\right\}-E^{(i,j)}=0,\ \ \forall j\in\mathcal{M}^{(i)}, \tag{24c}$$

$$\text{Im}\left\{W^{(i,j)}\right\}-F^{(i,j)}=0,\ \ \forall j\in\mathcal{M}^{(i)}, \tag{24d}$$

where

$$E^{(i,j)}-E^{(j,i)}=0,\ \ \forall j\in\mathcal{M}^{(i)}, \tag{24e}$$

$$F^{(i,j)}-F^{(j,i)}=0,\ \ \forall j\in\mathcal{M}^{(i)}. \tag{24f}$$

We leverage the relations in (24e) and (24f) when formulating the update rules of the distributed algorithm, but they are not enforced directly in the optimization problem. Note that the primary- and virtual secondary-side buses of a transformer cannot reside in two different areas. In our system model, we assume that the transformer t is attached at p_t, and that $\{p_t, s'_t\}$ are effectively the same physical bus; thus, its behavior is completely captured by $\mathcal{B}^{(i)}$ where $p_t\in\mathcal{A}^{(i)}$, and the boundary conditions will be enforced between buses s'_t and s_t.

A. Augmented Lagrangian

Let $\Gamma^{(i,j)}, \Lambda^{(i,j)} \in \mathbb{R}^{2\times 2}$ denote the Lagrange multipliers associated with the equality constraints in (24c) and (24d), respectively, where $c>0$ is the penalty coefficient. The augmented Lagrangian function for (24) is given in (25) at the top of this page, and is clearly separable amongst the three groups of variables such that

$$\mathcal{L}_c(\cdot)=\sum_{i\in\mathcal{P}}\mathcal{L}_c^{(i)}(\cdot). \tag{26}$$

Then, we can cyclically optimize the augmented Lagrangian $\mathcal{L}_c(\cdot)$ with respect to one of the groups of variables while holding the others constant with the following three-step update rule for the k^{th} iteration:

[S1.] *Primal Variables Update:* We take the infimum of $\mathcal{L}_c(\cdot)$ with respect to the primal variables, and update them as

$$W^{(i)}[k]=\underset{W^{(i)}\in\mathcal{B}^{(i)},\,W^{(i)}\succeq\mathbf{0}}{\arg\min}\ \mathcal{L}_c^{(i)}(\cdot), \tag{27}$$

which is dependent of the dual variables $\Gamma^{(i,j)}[k-1]$ and $\Lambda^{(i,j)}[k-1]$, and the boundary conditions $E^{(i,j)}[k-1]$ and $F^{(i,j)}[k-1]$.

[S2.] *Auxiliary Variables Update:* Recall that $E^{(i,j)}=E^{(j,i)}$ and $F^{(i,j)}=F^{(j,i)}$, also note that $\Lambda^{(i,j)}=-\Lambda^{(j,i)}$; then

$$\nabla_{E^{(i,j)}}\mathcal{L}_c(\cdot)=\text{Re}\left\{W^{(i,j)}+W^{(j,i)}\right\}-2E^{(i,j)}=0, \tag{28}$$

$$\nabla_{F^{(i,j)}}\mathcal{L}_c(\cdot)=\text{Im}\left\{W^{(i,j)}+W^{(j,i)}\right\}-2F^{(i,j)}=0. \tag{29}$$

We update the auxiliary variables with

$$E^{(i,j)}[k]=\frac{1}{2}\text{Re}\left\{W^{(i,j)}[k]+W^{(j,i)}[k]\right\}, \tag{30}$$

$$F^{(i,j)}[k]=\frac{1}{2}\text{Im}\left\{W^{(i,j)}[k]+W^{(j,i)}[k]\right\}, \tag{31}$$

for $j\in\mathcal{M}^{(i)}$.

[S3.] *Multipliers Update:* The gradient for the $\mathcal{L}(\cdot)$ with respect to the dual variables is

$$\nabla_{\Gamma^{(i,j)}}\mathcal{L}_c^{(i)}(\cdot) \ = \ \text{Re}\left\{W^{(i,j)}\right\}-E^{(i,j)}, \tag{32}$$

$$\nabla_{\Lambda^{(i,j)}}\mathcal{L}_c^{(i)}(\cdot) \ = \ \text{Im}\left\{W^{(i,j)}\right\}-F^{(i,j)}. \tag{33}$$

We initialize all the multipliers to zero; then, we solve the dual variables using an ascent method and apply (30)–(31). Thus, for $j\in\mathcal{M}^{(i)}$, the update rules for the dual variables are

$$\Gamma^{(i,j)}[k]=\Gamma^{(i,j)}[k-1]+\frac{c}{2}\text{Re}\left\{W^{(i,j)}[k]-W^{(j,i)}[k]\right\}, \tag{34}$$

$$\Lambda^{(i,j)}[k]=\Lambda^{(i,j)}[k-1]+\frac{c}{2}\text{Im}\left\{W^{(i,j)}[k]-W^{(j,i)}[k]\right\}. \tag{35}$$

Note that it follows naturally that $\Gamma^{(i,j)}=-\Gamma^{(j,i)}$ and $\Lambda^{(i,j)}=-\Lambda^{(j,i)}$.

Although Steps S1-S3 are formulated for the single-phase problem, they can easily be extended to solve three-phase unbalanced systems as well by accounting for all phase voltages per bus. The detailed extension is omitted here for brevity; however, the numerical results presented in the next section include this extension.

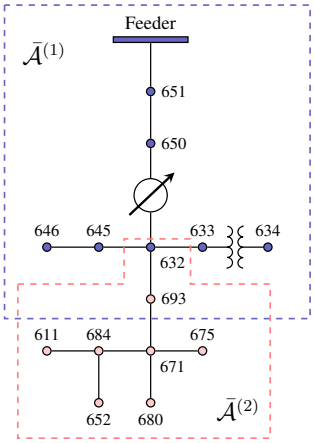

Figure 5: 15-Bus unbalanced distribution system.

V. Case Studies

In this section, we illustrate the ability of the distributed, ADMM-based algorithm proposed in Section IV to optimally set TCUL tap positions for both single- and three-phase cases of a 15-bus network. We also demonstrate the effectiveness of the algorithm on the IEEE 123-bus test system [19]. In all our studies, the voltage magnitude inequality constraints for all cases are limited to 1 p.u. $\pm$ 4.8%, rather than the common $\pm$ 5% to account for discrepancies associated with rounding to nearest discrete tap position.

We performed the simulations in MATLAB using the CVX package [22] with the symmetric cone solver SeDuMi [23]. This software package was used to solve the centralized problem and to update the primal variables $W^{(1)}, \ldots, W^{(L)}$ in step S1 of the distributed algorithm.

While in Section III-C we provided several penalty terms for different performance objectives, the cost function used in the case studies in Sections V-A and V-B only considers the distribution line losses as defined in (17), i.e., $f(W) = f_0(W)$.

A. 15-Bus Distribution System

We begin with the 15-bus network shown in Fig. 5, which we derived from the IEEE 13-bus—a three-phase, unbalanced distribution system, (see, e.g., [1], [19]). The system has a three-phase voltage regulation transformer between buses 650 and 632. The rest of the system contains single-, two-, and three-phase sublaterals. Buses 650 and 651 were added between the feeder and the transformer so that the transformer was not directly connected to the slack bus. Bus 693 was added to account for the distributed load along line (632, 671), and bus 692 was removed since it corresponds to a closed switch connected between buses 671 and 675.

In Fig. 5, busses are color coded for areas $\mathcal{A}^{(1)}$ and $\mathcal{A}^{(2)}$; the extended areas $\bar{\mathcal{A}}^{(1)}$ and $\bar{\mathcal{A}}^{(2)}$ are distinguished by the dashed lines circling the areas. The overlap occurs at buses 632 and 693 where $W^{(1,2)} \in \mathbb{C}^{2\times 2}$ for the 14-bus single-phase case and $W^{(1,2)} \in \mathbb{C}^{6\times 6}$ for the following three-phase case.

1) Single-Phase Results: For the single-phase system, we isolate phase C from Fig. 5 since it is the dominant phase of the 15-bus network, and create a 14-bus single-phase case that excludes bus 652 from the network topology since phase C is not present on that bus. The results obtained using: (i) a centralized algorithm, (ii) our distributed algorithm, and (iii) an exhaustive search where we enumerate all of the possible tap ratio combinations are shown in Table I. All three methods return the same optimal tap position. The exhaustive search uses an ideal transformer model and the difference in the cost function $f(W)$ compared to the other two methods is due to the loss S_t through the non-ideal transformer model. Figures 6(a) and 6(b) show the evolution of the area cost functions and the corresponding tap ratio for $c = 60$. Notice that the optimal position occurs near iteration 250 where the global $f(W)$ remains relatively unchanged after iteration 125, so there are several tap ratios that will result in acceptable

Table I: Single-Phase 14-Bus Network

	Centralized OPF	Distributed OPF	Exhaustive Search
$f(W)$	0.559	0.466, 0.094	0.554
$\lvert V_{p_t}\rvert$	1.007	1.007	1.007
$\lvert V_{s'_t}\rvert$	1.060	1.060	–
$\lvert V_{s_t}\rvert$	1.048	1.048	1.048
$S_{p_t s'_t}$	$11.05 + j4.01$	$11.04 + j4.01$	–
S_t	0.005	0.005	–
Tap	-8	-8	-8
CPU Time	0.8 s	–	0.1 s

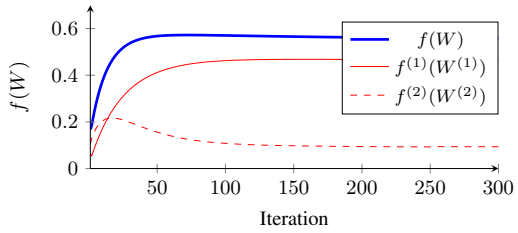

(a) Objective Functions

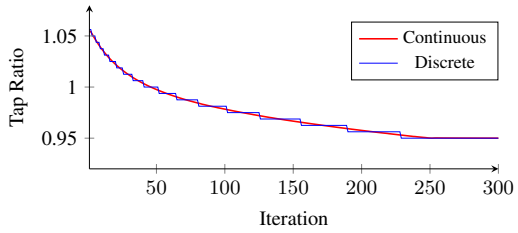

(b) Tap position

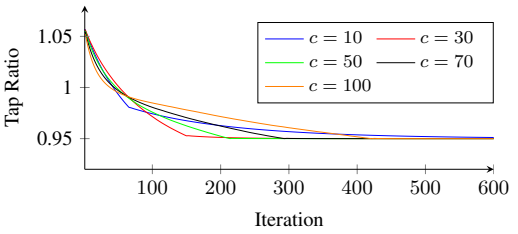

(c) Convergence for Various Penalty Parameters

Figure 6: 14-bus, single-phase results.

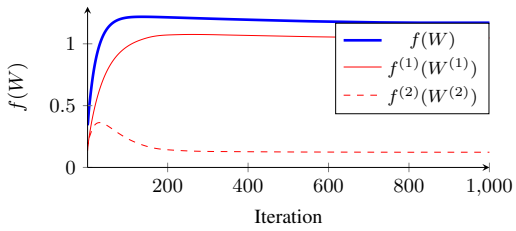

(a) Objective Functions

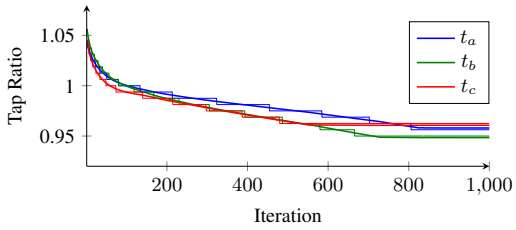

(b) Tap position

Figure 7: 15-bus, three-phase results.

Table II: THREE-PHASE 15-BUS NETWORK

	Centralized OPF	Distributed OPF	Exhaustive Search	Power Flow
$f(W)$	1.170	1.047, 0.123	1.170	1.167
$\lvert V_{p_t}\rvert$	1.028 1.017 1.023	1.028 1.017 1.023	1.028 1.017 1.023	1.028 1.017 1.023
$\lvert V_{s'_t}\rvert$	1.073 1.073 1.064	1.073 1.073 1.064	– – –	– – –
$\lvert V_{s_t}\rvert$	1.048 1.044 1.043	1.048 1.044 1.043	1.043 1.042 1.041	1.050 1.042 1.041
$S_{p_t s'_t}$	$8.5+j4.1$ $9.6+j4.7$ $9.8+j3.3$	$8.5+j4.1$ $9.6+j4.7$ $9.8+j3.3$	– – –	– – –
S_t	0.004	0.004	–	–
Tap	-7, -8, -6	-7, -8, -6	-6, -8 , -6	-7, -8, -6
CPU Time	2.0 s	–	107.2 s	–

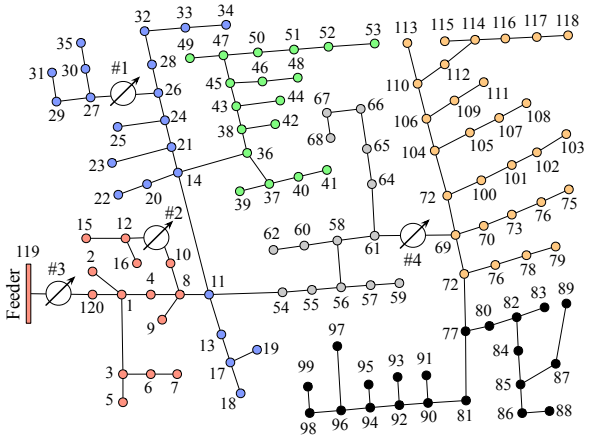

Figure 8: IEEE 123-bus distribution system.

solutions. Figure 6(c) shows the effect of changing the penalty parameter c. For the 14-bus network, the fastest convergence occurs when $c \approx 30$.

2) Three-Phase Results: In the centralized case, the 15-bus, three-phase unbalanced system problem will have 1763 optimization variables since $W \in \mathbb{C}^{41\times 41}$. In contrast, the distributed case has a 21.8% reduction for a combined total of 1379 variables (910 for area 1 and 469 for area 2). The results for the three-phase case are listed in Table II with the progress of the distributed algorithm displayed in Fig. 7. The solutions to the relaxed problem (incorporating the non-ideal transformer model) obtained with the centralized and distributed solvers yielded the same tap positions of $\{-7,-8,-6\}$. The exhaustive search solution yielded a different result for phase A, with the final tap positions being $\{-6,-8,-6\}$. However, if we check the centralized and distributed result by solving the power flow equations, we found the solution to be acceptable. Similar to the single-phase case, there are several solutions around the selected tap positions with nearly the same costs for the objective function.

From the results in Table I, we can see that the exhaustive search method for a single tap resulted in a faster computation than the relaxed centralized problem, with CPU times of 0.1 s versus 0.8 s, respectively. In the three-phase case, the added computational complexity introduced by the dimensional increase associated with the additional phases resulted in an increase of the CPU time for the exhaustive search solution to 107.2 s, while the relaxed centralized case increased slightly to 2.0 s. The ADMM-based solution that we proposed was tested using a serial implementation on a single-core; thus, we intentionally did not include the CPU time for this case, we refer the reader to [9], [15], [16] for computational benefits of ADMM.

B. 123-Bus Distribution System

Figure 8 shows the one-line diagram for the IEEE 123-bus, three-phase distribution system, which includes four three-phase voltage regulation transformers [19]; we also divide the system into six areas. This is a comprehensive system that is mostly unbalanced and contains overhead/underground distribution line segments with single-, two-, and three-phase branches. We set the voltage at the feeder to 1.01 p.u. so that there are 18 buses experiencing an under-voltage with the worst being 0.937 p.u. on bus 118. Note that for this particular case, we did not include results for an exhaustive search of the transformer tap settings since the number combinations with the hardware available is 33^9. Therefore we can not obtain a solution in a reasonable amount of time. In contrast, the centralized convex relaxation took 71.5 s of CPU time to reach the solution.

In this case, we have that $W \in \mathbb{C}^{259\times 259}$ and the centralized relaxed OPF has 268,854 optimization variables. The centralized algorithm yielded a solution such that the tap positions are in the neutral position for regulators 1 and 2, are set to $\{-5,-1,-3\}$ for regulator 3, and are set to $\{-2,-1,-1\}$

for regulator 4. The minimum voltage is raised to 0.985 p.u. and the network losses are 0.8286 p.u. The bus voltage error between the continuous and the rounded discrete tap positions has an average of 6.63×10^{-4} p.u. and a standard deviation of 0.0017 p.u. with a maximum error of 0.0029 p.u.

In contrast, the distributed algorithm results in 59,436 optimization variables, which is a 77.89% reduction from the centralized scheme. The distributed method returned slightly different results for the tap positions: regulators 1 and 2 taps are set to the neutral position, regulator 3 taps are set to $\{-4, -1, -2\}$, and regulator 4 taps are set to $\{0, 1, 0\}$. The minimum voltage in this configuration is 0.965 p.u. on bus 118. However, the minimum computed network losses for this configuration are 0.8303 p.u., which represents a 0.3% difference from the centralized result. For this particular network and loading, the tap positions of regulator 3 impact the network conditions the most since this transformer is connected to the feeder. As the number of transformers on the network increases, there could be multiple solutions that minimize the cost function.

C. Impact of the Choice of z_t

Next, we explore the impact of the z_t on the solution of the 15-bus, unbalanced three-phase optimization; the results are captured in Fig. 9. In each subfigure, the thick red vertical line represents the resistance of the neighboring distribution line segments with the vertical lines to the left and right represent approximately an order of magnitude less and every two orders of magnitude larger, respectively.

The objective function for this particular case is of the form

$$f(W) = f_0(W) + \sum_{i \in \mathcal{N}} (1 - [W]_{ii})^2, \tag{36}$$

where the summation term penalizes the voltage deviations from 1 p.u. Figure 9(a) shows the optimization variables $S_{p_t s'_t}$ for the power transferred through the transformer and the phase difference $\theta_{p_t} - \theta_{s'_t}$ between the primary and secondary sides of the transformer versus the impedance of z_t. In Fig. 9(b) we plot the power transferred through z_t and the rank of the W returned from the convex optimization. In Fig. 9(c) we show cost function $f(W)$ and the normalized percent error

$$e\left(W, V(a_t)\right) = 100 \sqrt{\sum_{i \in \mathcal{N}} \left(\frac{\sqrt{[W]_{ii}} - V_i(a_t)}{V_i(a_t)} \right)^2}, \tag{37}$$

which is determined by the difference between the voltage magnitudes recovered from $W(z_t)$ and the voltage magnitudes shown in Fig. 9(d) that are computed from the power flow with rounded discrete tap positions.

In Section III-B, we proposed to choose $|z_t|$ several orders of magnitude larger than the impedance of the adjacent distribution line segments. For the 15-bus system, the optimization solution tends to match the power flow results better for small values of z_t, the desired results were captured when z_t is chosen such that $|z_t|$ is two to four orders of magnitude larger than the magnitude of the impedance of neighboring distribution lines. Within this interval, the power transferred

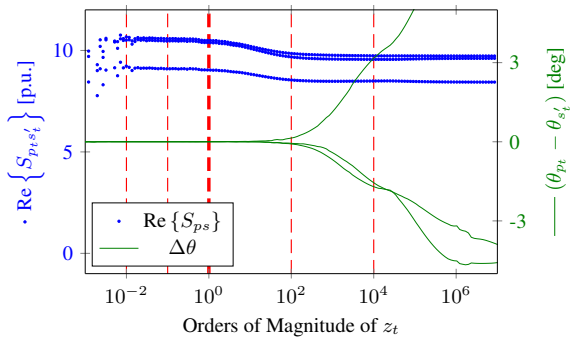

(a) Power transferred through $S_{p_t s'_t}$ and phase mismatch between p_t and s'_t versus $|z_t|$.

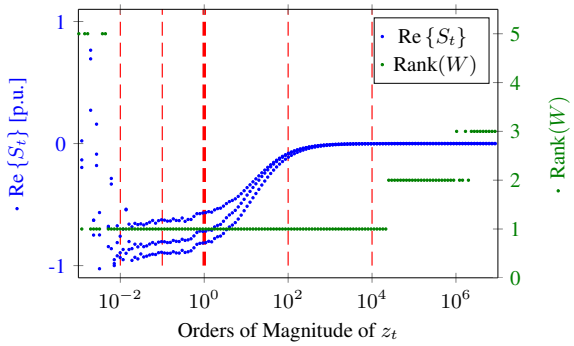

(b) Power transferred through z_t and the rank of W.

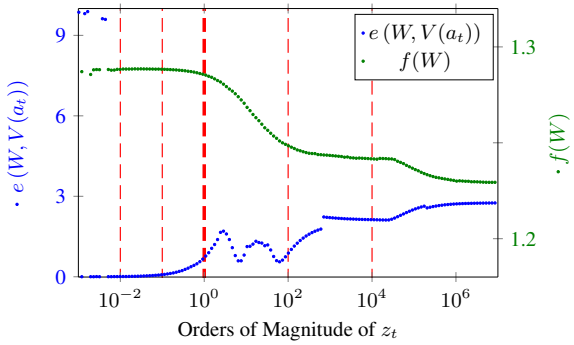

(c) Normalized percentage of the voltage error and the objective function in the form $f(W) = f_0(W) + f_2(W)$.

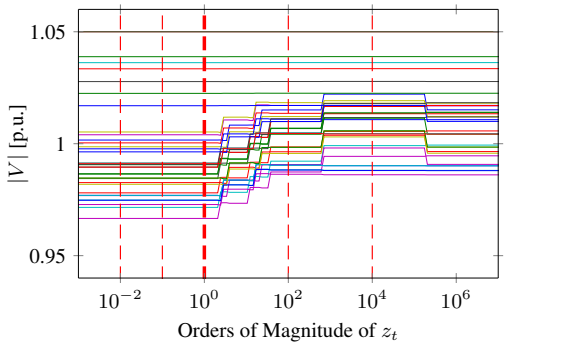

(d) Power flow results for bus voltages from rounded tap positions.

Figure 9: The effects of the choice of z_t on the optimization results for the 15-bus unbalanced distribution system.

through z_t converges to zero and the system values in the optimization converge to a steady-state. We also see that the rank of W is still one with a subtle discrepancy in the angle difference across the transformer of less than 3 degrees and a normalized voltage magnitudes error of less than 2% between the power flow results and the resulting $W(z_t)$. After four orders of magnitude difference, the system behaves as the disconnected case and we are no longer able to accurately recover the solution. Note that these results are for this specific case. In other scenarios we have found that by choosing $|z_t|$ approximately two orders of magnitude larger than the neighboring distribution line segments is a good initial value.

VI. Concluding Remarks

In this paper, we developed a method to optimally set, via a distributed ADMM-based algorithm, tap positions of voltage regulation transformers in distribution systems. We demonstrated the applicability of this method via numerical examples involving single- and three-phase test systems.

Future work will include improving the convergence of the distributed ADMM-based algorithm. We also intend to apply this distributed optimization approach to a system-wide voltage tracking control scheme. In this case, we would periodically dispatch the TCUL transformers and then draw upon our previous work in [18] to handle fast-transients that can be corrected with reactive power support.

Appendix

A. Notation

$\mathcal{T}$	Set of transformers indexed $\{1,\dots,r\}$
a	Set of transformer tap ratios indexed $\{a_1,\dots,a_r\}$
$\mathcal{N}_p$	Set of bus incident to the primary side of a transformer indexed $\{p_1,\dots,p_r\}$
$\mathcal{N}_s$	Set of bus incident to the secondary side of a transformer indexed $\{s_1,\dots,s_r\}$
$\mathcal{N}_{s'}$	Set of bus incident to the virtual secondary side of a transformer indexed $\{s'_1,\dots,s'_r\}$
$\mathcal{N}_b$	Set of buses not incident to a transformer
$\mathcal{N}$	Set of physical buses
$\mathcal{N}_a$	Augmented set of buses that includes $\mathcal{N}_{s'}$
S_{ps}	Set of transformer power transfers indexed $\{S_{p_1 s'_1},\dots,S_{p_r s'_r}\}$
z_t	Impedance added for the non-ideal transformer model
W	Semi positive-definite matrix of bus voltages
$W^{(i,j)}$	Submatrix of $W^{(i)}$ boundary conditions with neighbor j
$E^{(i,j)}$	Auxiliary variable associated with $\mathrm{Re}\{W^{(i,j)}\}$
$F^{(i,j)}$	Auxiliary variable associated with $\mathrm{Im}\{W^{(i,j)}\}$
$\mathcal{P}$	Set of partitions indexed $1,\dots,L$
$\mathcal{A}^{(i)}$	Set of buses in the area defined by $i \in \mathcal{P}$
$\bar{\mathcal{A}}^{(i)}$	The extended area containing neighboring buses
$\mathcal{M}^{(i)}$	The partitions neighboring i
$\mathcal{B}^{(i)}$	The set of power flow constraints and inequalities for partition i
$\mathcal{L}_c(\cdot)$	The augmented Lagrangian with penalty parameter c
$\Gamma^{(i,j)}$	Boundary condition dual variable for $\mathrm{Re}\{W^{(i,j)}\}$
$\Lambda^{(i,j)}$	Boundary condition dual variable for $\mathrm{Im}\{W^{(i,j)}\}$

References

[1] W. H. Kersting, *Distribution System Modeling and Analysis*. New York, NY: CRC Press, 2001.

[2] P. W. Sauer and M. A. Pai, "A comparison of discrete vs continuous dynamic models of tap-changing-under-load transformers," in *Proc. Bulk Power System Voltage Phenomena III: Voltage Stability, Security, & Control*, Davos, Switzerland, Aug 1994.

[3] W.-H. E. Liu, A. D. Papalexopoulos, and W. F. Tinney, "Discrete shunt controls in a newton optimal power flow," *IEEE Trans. on Power Systems*, vol. 7, no. 4, pp. 1509–1518, 1992.

[4] E. Acha, H. Ambriz-Perez, and C. R. Fuerte-Esquivel, "Advanced transformer control modeling in an optimal power flow using newton's method," *IEEE Trans on Power Systems*, vol. 15, no. 1, pp. 290–298, 2000.

[5] M. M. Adibi, R. A. Polyak, I. A. Griva, L. Mili, and S. Ammari, "Optimal transformer tap selection using modified barrier-augmented lagrangian method," in *Proc. IEEE Power Engineering Society General Meeting*, vol. 2, 2003.

[6] S. Bose, D. F. Gayme, S. H. Low, and K. M. Chandy, "Optimal power flow over tree networks," in *Proc. of Allerton Conf. on Comm., Control, & Computing*, 2011, pp. 1342–1348.

[7] B. Zhang, A. Lam, A. Domínguez-García, and D. Tse, "An optimal and distributed method for voltage regulation in power distribution systems," *IEEE Trans. on Power Systems*, 2014.

[8] J. Lavaei, D. Tse, and B. Zhang, "Geometry of power flows in tree networks," in *Proc. IEEE Power and Energy Society General Meeting*, 2012, pp. 1–8.

[9] E. Dall'Anese, H. Zhu, and G. Giannakis, "Distributed optimal power flow for smart microgrids," *IEEE Trans. on Smart Grid*, vol. 4, no. 3, pp. 1464–1475, Sept 2013.

[10] R. A. Jabr, "Optimal power flow using an extended conic quadratic formulation," *IEEE Trans. on Power Systems*, vol. 23, no. 3, pp. 1000–1008, Aug 2008.

[11] J. Lavaei, "Zero duality gap for classical opf problem convexifies fundamental nonlinear power problems," in *Proc. American Control Conference (ACC)*, 2011, pp. 4566–4573.

[12] B. A. Robbins, H. Zhu, and A. D. Dominguez-Garcia, "Optimal tap settings for voltage regulation transformers in distribution networks," in *Proc. 2013 North American Power Symposium (NAPS)*, 2013, pp. 1–6.

[13] J. Lavaei and S. H. Low, "Convexification of optimal power flow problem," in *Proc. 48th Allerton Conf. on Communication, Control, & Computing*, 2010, pp. 223–232.

[14] J. Lavaei and S. H. Low, "Zero duality gap in optimal power flow problem," *IEEE Trans on Power Systems*, vol. 27, no. 1, pp. 92–107, 2012.

[15] M. Kraning, E. Chu, J. Lavaei, and S. Boyd, "Dynamic network energy management via proximal message passing," *Foundations and Trends in Optimization*, vol. 1, no. 2, pp. 1–54, 2013.

[16] S. Boyd, N. Parikh, E. Chu, B. Peleato, and J. Eckstein, "Distributed optimization and statistical learning via the alternating direction method of multipliers," *Foundations and Trends in Machine Learning*, vol. 3, no. 1, pp. 1–122, 2011.

[17] H. Zhu and G. B. Giannakis, "Multi-area state estimation using distributed sdp for nonlinear power systems," in *Proc. of IEEE Converence on Smart Grid Communications*, Nov 2012, pp. 623–628.

[18] B. A. Robbins, C. N. Hadjicostis, and A. D. Dominguez-Garcia, "A two-stage distributed architecture for voltage control in power distribution systems," *IEEE Trans on Power Systems*, vol. 28, no. 2, pp. 1470–1482, May 2013.

[19] IEEE Power and Energy Society. (2010, Sept) Distribution test feeders. [Online]. Available: http://www.ewh.ieee.org/soc/pes/dsacom/testfeeders/index.html

[20] E. Dall'Anese, S. Dhople, and G. B. Giannakis, "Optimal dispatch of photovoltaic inverters in residential distribution systems," *arXiv:1307.3751*, 2014.

[21] Y. Ye, "Linear conic programming," Dec 2004, Stanford MS&E314/ CME336 Course Notes.

[22] S. Boyd, "Cvx: Matlab software for disciplined convex programming," Mar 2014. [Online]. Available: http://cvxr.com/cvx/

[23] CORAL Lab, "Sedumi," Mar 2014. [Online]. Available: http://sedumi.ie.lehigh.edu

Brett A. Robbins (S'07) received his B.S. and M.S. degrees in electrical engineering from the University of Illinois at Urbana-Champaign in 2008 and 2011, respectively. Currently, he is pursuing the Ph.D. degree from the University of Illinois at Urbana-Champaign. His research interests include the modeling, simulation, and control of power systems, and the integration and control of distributed energy resources.

Hao Zhu (M'12) is an Assistant Professor of ECE at the University of Illinois, Urbana-Champaign (UIUC). She received her B.S. from Tsinghua University, Beijing, China in 2006, and the M.Sc. and Ph.D. degrees from the University of Minnesota, Minneapolis in 2009 and 2012, respectively. She has been working as a postdoctoral research associate on power system validation with the Information Trust Institute at UIUC 2012-2013. Her current research interests include power system monitoring and operations, dynamics and stability, distribution systems, and energy data analytics.

Alejandro D. Domínguez-García (S'02, M'07) received the degree of Electrical Engineer from the University of Oviedo (Spain) in 2001 and the Ph.D. degree in electrical engineering and computer science from the Massachusetts Institute of Technology, Cambridge, MA, in 2007.

He is an Associate Professor in the Electrical and Computer Engineering Department at the University of Illinois at Urbana-Champaign, where he is affiliated with the Power and Energy Systems area; he also has been a Grainger Associate since August 2011. He is also an Associate Professor in the Coordinated Science Laboratory and in the Information Trust Institute, both at the University of Illinois at Urbana-Champaign. His research interests are in the areas of system reliability theory and control, and their applications to electric power systems, power electronics, and embedded electronic systems for safety-critical/fault-tolerant aircraft, aerospace, and automotive applications.

Dr. Domínguez-García received the NSF CAREER Award in 2010, and the Young Engineer Award from the IEEE Power and Energy Society in 2012. He is an editor of the IEEE TRANSACTIONS ON POWER SYSTEMS and the IEEE POWER ENGINEERING LETTERS.